energies

MDPI

Article

Sensitivity Analysis of Steel-Plate Concrete Containment against a Large Commercial Aircraft

Xiuyun Zhu [1,2,*], Jianbo Li [1], Gao Lin [1], Rong Pan [2] and Liang Li [2]

[1] Faculty of Infrastructure Engineering, Dalian University of Technology, Dalian 116024, China; jianboli@dlut.edu.cn (J.L.); gaolin@dlut.edu.cn (G.L.)
[2] Nuclear and Radiation Safety Center, Ministry of Ecology and Environment, Beijing 100082, China; panrong@chinansc.cn (R.P.); liliang@chinansc.cn (L.L.)
* Correspondence: zhuxiuyun@chinansc.cn or lyzhuxiuyun@163.com

Abstract: Due to the excellent impact resistant performance of steel-plate concrete (SC) structure compared with the conventional reinforced concrete (RC) structure, SC structure is preferred to be used in the design of external walls of nuclear island buildings for new nuclear power plants (NPPs). This study aims at evaluating the effect of material and geometric parameters of SC containment on its impact resistant performance, thus the numerical simulation and sensitivity analysis of SC containment subjected to malicious large commercial aircraft attack are conducted based on the force time-history analysis method. The results show that: (1) the impact resistant performance of full SC containment is better than that of half SC containment; (2) for relatively thin full SC containment, the impact response and concrete damage can be significantly reduced by the enhancing of concrete strength grade or the increasing of steel plate thickness; (3) for the thicker full SC containment, concrete strength grade has only a slight influence on the impact displacement response, and the increasing of steel plate thickness has no significant effect on mitigating the impact displacement response. However, the increasing of steel plate thickness can effectively reduce its plastic strain, and the decreasing of strength grade of steel plate may obviously increase its plastic strain; and (4) concrete thickness plays a decisive role on the improvement of impact resistance, which is more effective than the enhancing of concrete strength grade. Resultantly, this paper provides a reference and guidance for the design of SC structure external walls of nuclear island buildings against a large commercial aircraft.

Keywords: impact dynamics; steel-plate concrete (SC) containment; sensitivity analysis; force time-history analysis method; large commercial aircraft impact

Citation: Zhu, X.; Li, J.; Lin, G.; Pan, R.; Li, L. Sensitivity Analysis of Steel-Plate Concrete Containment against a Large Commercial Aircraft. *Energies* **2021**, *14*, 2829. https://doi.org/10.3390/en14102829

Academic Editor: Rosa Lo Frano

Received: 11 April 2021
Accepted: 10 May 2021
Published: 14 May 2021

1. Introduction

After the 9/11 incident, nuclear power plants (NPPs) against malicious impact of a large commercial aircraft has become a significant focus of nuclear safety. Under these circumstances, the U.S. Nuclear Regulatory Commission (NRC)'s regulations issued in 2009 required licensee to perform a specific assessment regarding the impact of a large commercial aircraft on the facility as a beyond design basis event [1]. Technology guidance of NEI 07-13 [2] provided an acceptable method to satisfy NRC's regulations of 10 CFR 50.150. Using realistic analyses, applicants must identify and incorporate into the design, and those design features and functional capabilities to show that the reactor core remains cooled or the containment remains intact with reduced use of operator actions. For the non-linear dynamic analysis, global structure response of the target structure can be evaluated based on force time-history analysis method or missile-target interaction analysis method. China's nuclear safety regulation of HAF102 [3] specified the relevant requirement for NPP to resist the malicious commercial aircraft attack, which clearly stated that, if the terrain conditions of NPP location made it possibly to suffer the malicious impact of commercial

aircraft, the assessment of such impact should be considered as a beyond design basis event.

In the 1960s, Riera [4] proposed a simplified theory model for force time-history analysis method based on the reaction versus time relationship of the aircraft impact against a rigid wall. Subsequently, extensive experimental and analytical research work has been performed on impact analysis of reinforced concrete (RC) structure against intentional aircraft crash by domestic and abroad researchers for last several decades [5–9]. Jiang and Chorzepa [10] reviewed the available numerical and experimental studies and summarized the investigation which may be used to benchmark an aircraft impact simulation. Kyoungsoo et al. [11] presented that the results of nonlinear dynamic analyses of prestressed concrete containment under the impact of a large commercial aircraft Boeing 747 based on missile-target interaction analysis method. Preliminary evaluation of military and civil aircrafts impact on a near term NPP was conducted using the force time-history analysis method [12]. The global and local structural safety of a nuclear auxiliary building under the crash of Boeing 767-400 was ensured with regard to different impact scenarios [13]. Aircraft impact analysis of primary auxiliary buildings was performed, and floor response spectra and the structure integrity of the external wall against aircraft impact were analyzed [14]. The above studies were all aimed at RC structure, whereas the impact resistance of steel-plate concrete (SC) structure was studied relatively few. Mullapudi et al. [15] conducted a series of numerical studies to evaluate the effect of several parameters affecting the behavior of SC walls based on force time-history analysis method. Parametric study was performed to investigate the influences on the damage to the SC structure shield building subjected to attack of Boeing 767-200ER [16]. Sadiq et al. [17] investigated the effectiveness of multiple barriers employed in safety-related RC and SC structures of NPPs against aircraft impact. Sadiq et al. [18] carried out the simulation analysis of 1/7.5 scale model impact tests of SC and RC panels with different thickness against aircraft crash [19,20], and the analytical results correlated well with the test results and exhibited that SC structure was more effective than RC structure against aircraft impact. Therefore, due to the excellent impact resistant performance, SC structure was preferred in the design of external walls of nuclear island buildings for new NPPs. For example, structure type of AP1000 shield building had been changed to SC structure from RC structure by considering the resistance of a large commercial aircraft impact [21].

In this study, in order to further investigate the influence of material and geometric parameters of SC containment on its impact resistance, as the first step, numerical analysis aimed at evaluating the impact resistant behavior of full SC and half SC containment against a large commercial aircraft is conducted. Simulation results in terms of impact displacement, plastic strain, concrete damage, internal energy, and total energy absorbed are compared and analyzed comprehensively. Subsequently, sensitivity analysis of different strength grade and thickness for concrete and steel plate of full SC containment on its impact resistance is carried out.

2. Numerical Analysis Method and Models

2.1. Impact Force Time-History Function

For the force time-history analysis method, the impact force time-history function is firstly determined based on the aircraft crushing strength information and impulse conservation principles. Riera [4] proposed an equation to calculate the impact force of an aircraft normally impacting rigid wall, as follows:

$$F(t) = P_c(x(t)) + \mu(x(t))v^2(t), \quad (1)$$

where $F(t)$ is the total impact force, $P_c(x(t))$ is the crushing force located at coordinate $x(t)$, $\mu(x(t))$ is the mass per unit length at location $x(t)$, and $v(t)$ is the residual velocity of the uncrushed portion. As shown in Equation (1), the total impact force is the combination of the crushing force and the inertial force against the rigid target. In this paper, the impact force time-history function of a large commercial aircraft Boeing 747 is selected as shown

in Figure 1 [22], which the first peak is due to the crushing of airplane fuselage, while the second much more severe peak is related to the impact of fuselage and the much more stiff engines, and, after that, only the fuselage load is continued until the end. Therefore, according to the character of commercial aircraft, the impact effect can be divided by two parts of fuselage and two wings, which the action area of each part is 50 m^2 [22]. The time varying uniform impact pressure for fuselage and two wings can be obtained as shown in Figure 2.

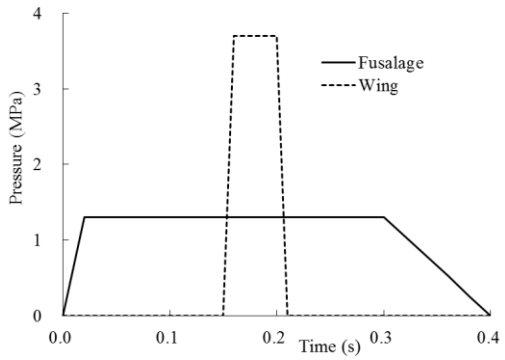

Figure 1. The impact force time-history function of Boeing 747 [22].

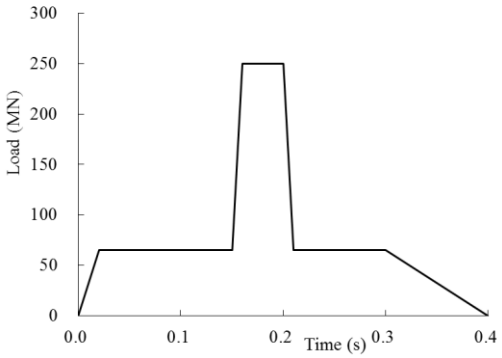

Figure 2. The impact pressure time-history function of fuselage and wing [22].

2.2. Finite Element Model

Generally, SC structure is usually divided as two types, which are full SC and half SC. Full SC structure has steel plate on both faces of the structural component, and composite action is provided by headed stud anchors embedded in concrete. Half SC structure has steel plate on one side only and rebar on the other side as conventional RC structure. Of course, for half SC structure, steel plate can be selected to be placed on the inside or outside according to the requirement. In this study, total of three models are considered, which the model I represents full SC containment, the model II and model III are both half SC containment. The model II represents steel plate placed on the outer face of containment, and rebar located on the inner side, while the model III represents steel plate placed on the inner face of containment, rebar located on the outer side.

Containment usually consists of raft foundation, cylinder and dome. The geometrical dimension of SC containment is as follows: the total height is 67.2 m, the outer diameter and height of cylinder is 51.2 m and 55.8 m. Due to sensitivity analysis of geometric parameters, the thickness of cylinder and dome is 0.8–1.1 m, and the thickness of the inner and outer steel plate is the same and 16–22 mm for full SC containment. The diameter and space of rebar for half SC containment is 40 mm and 200 mm, respectively. Due to the symmetry of containment structure and crash zone, half model of SC containment is built by nonlinear finite element (FE) code of ANSYS/LS-DYNA (Ansys Inc., Canonsburg, PA, USA) [23]. To avoid negative volume effect, concrete is modeled by 8-nodes constant stress

solid element Solid164, which is divided into four layers along the thickness direction, and the size along the other directions is about 0.6 m × 0.67 m and 0.3 m × 0.67 m. Steel plate is modeled by 4-nodes Belytschko–Tsay shell element Shell163. For half SC containment, rebar is modeled in discrete manner by three nodes beam element Beam161 with Hughes-Liu element formulation. These reinforcing beams are coupled with solid concrete elements via coupling constraint of *CONTRAINED_LAGRANGEIN_IN_SOLID which provides coupling mechanism for two different elements without sharing common nodes [23]. Connection between steel plate element and the contact surface of concrete element is created by common nodes, so that the steel plate is glued to the concrete surface with strain compatible.

The FE model of full SC and half SC containment is shown in Figures 3 and 4, respectively. For load application of the half model, the center zone on the middle of the cylinder, where the impact pressure applied is illustrated in Figure 3a,b. The area of half fuselage and one wing is 25 m^2, respectively. The impact pressure of fuselage and wing as shown in Figure 2 is separately applied to these corresponding elements as shown in Figure 5. The total number of elements and nodes in the FE models of model I, model II, and model III is summarized in Table 1. For the boundary condition, fixed boundary at the bottom of raft foundation is applied by restraining translation degrees of freedom along the three orthogonal directions (i.e., UX, UY, UZ); meanwhile, the symmetric degree of freedom (i.e., UX, ROTY, ROTZ) is restrained at the symmetric plane, as shown in Figure 3c.

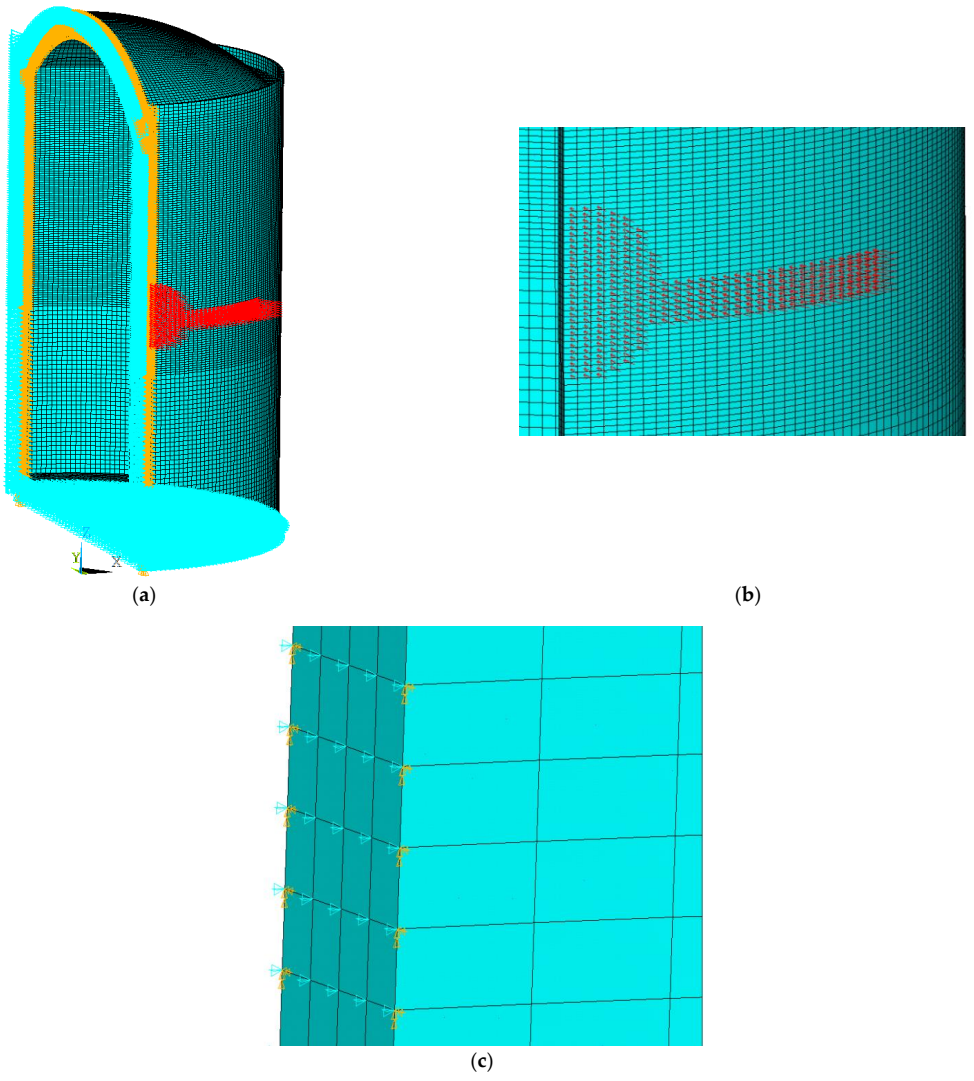

Figure 3. Finite element model of full SC containment. (**a**) Overall model; (**b**) Load area; (**c**) Symmetric restriction.

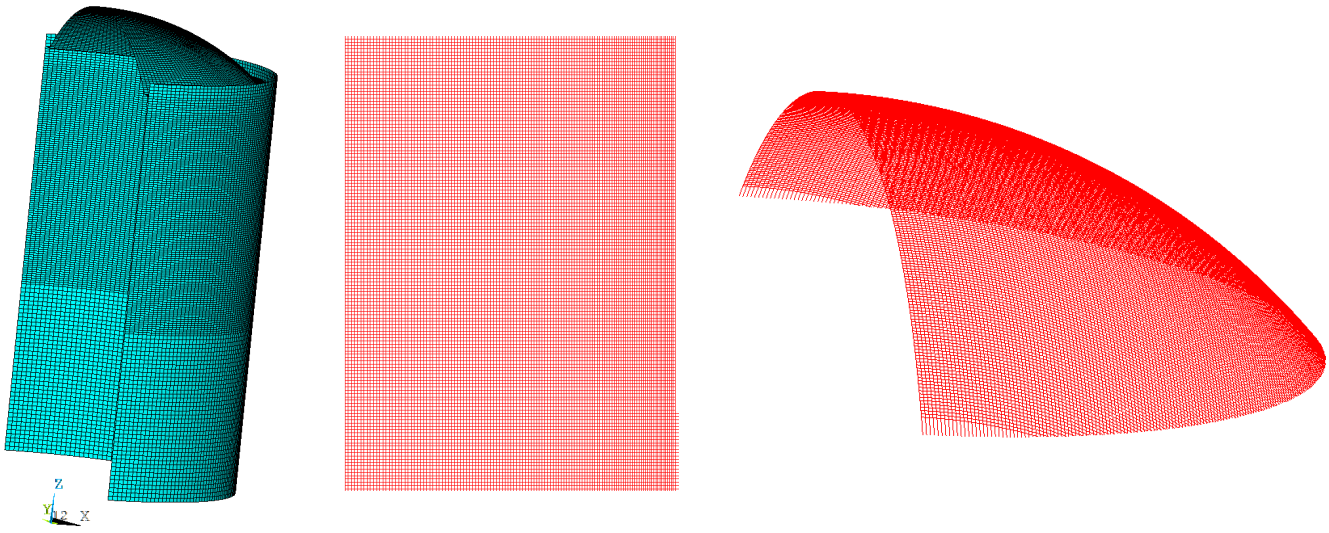

Figure 4. Finite element model of half SC containment. (**a**) Steel plate; (**b**) Rebar of cylinder; (**c**) Rebar of dome.

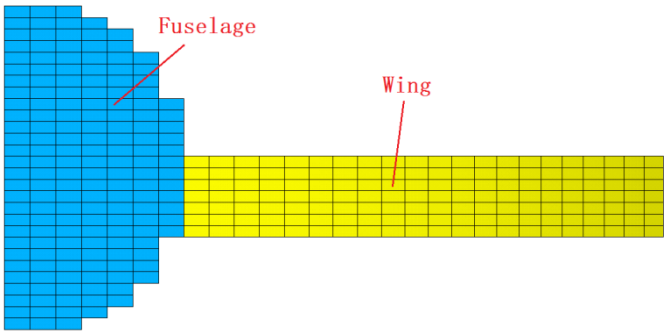

Figure 5. Crash zone of fuselage and wing.

Table 1. Total number of elements and nodes.

Model	Solid Elements	Shell Elements	Beam Elements	Nodes
I	102,018	48,720	/	129,182
II	102,018	24,840	114,533	337,470
III	102,018	23,880	115,905	340,214

2.3. Numerical Material Models

To realistically predict the behavior of SC structure under impact load, it is necessary to study the nonlinear constitutive model and failure criterion. Nonlinear FE code of ANSYS/LS-DYNA provides various material models developed for specific applications which require an appropriate set of input parameters [23].

2.3.1. Concrete Constitutive Model

The ANSYS/LS-DYNA is widely applied in analyzing structural responses to shock and impact loads and provides a variety of concrete constitutive models. Although each of these models has its own advantages and disadvantages, the Winfrith concrete model (*MAT_WINFRITH_CONCRETE) was developed in solving RC structure subjected to impact loadings and was implemented into ANSYS/LS-DYNA in 1991 [23]. The Win-

frith concrete model was based upon the so called four parameter model proposed by Ottosen [24]. The yield function can be written as:

$$Y(I_1, J_2, J_3) = aJ_2 + \lambda\sqrt{J_2} + bI_1 - 1, \tag{2}$$

where, I_1 is the 1st invariant of stress tensor, which represents volumetric responses; J_2 and J_3 are the 2nd and 3rd invariants of deviatoric stress tensor, respectively; λ is calculated as follows:

$$\lambda = \begin{cases} k_1 \cos\left[\frac{1}{3}\cos^{-1}(k_2\cos(3\theta))\right] & , \quad \cos(3\theta) \geq 0 \\ k_1 \cos\left[\frac{\pi}{3} - \frac{1}{3}\cos^{-1}(-k_2\cos(3\theta))\right] & , \quad \cos(3\theta) \leq 0 \end{cases} \tag{3}$$

where, the calculation of $\cos(3\theta)$ is shown in Equation (4)

$$\cos(3\theta) = \frac{3\sqrt{3}}{2}\frac{J_3}{J_2^{3/2}} \tag{4}$$

The four parameters, i.e., a, b, k_1, and k_2, are functions of the ratio of tensile strength to compressive strength f_t/f_c', and they are determined from uniaxial compression (correspondingly, $\theta = 60^\circ$), uniaxial tension ($\theta = 0^\circ$), biaxial compression ($\theta = 0^\circ$), and triaxial compression ($\theta = 60^\circ$) tests. Where, the calculation of $\cos(3\theta)$ is shown in Equation (4).

For the failure criterion, the prediction of concrete failure is a difficult task due to complex nature of concrete as it exhibits both ductile and brittle failure. In ANSYS/LS-DYNA, *MAT_ADD_EROSION option provides a way of controlling material failure. The damaged element is removed from the model when the damage variable reaches the predetermined critical value. Since the strength of concrete changes with strain rate, and the concrete is mainly damaged for pressure under impact load, the maximum principal strain is chosen as the failure criterion of concrete.

2.3.2. Steel Constitutive Model

Cowper-Symonds constitutive model which is corresponding to *MAT_PLASTIC_KINEMATIC from ANSYS/LS-DYNA material library is suited to model isotropic and kinematic hardening plasticity with the option of including rate effect [22]. The yield stress is written as:

$$\sigma_y = \left[1 + \left(\frac{\dot{\varepsilon}}{C}\right)^{\frac{1}{p}}\right]\left(\sigma_0 + \beta E_p \varepsilon_p^{eff}\right) \tag{5}$$

where $\dot{\varepsilon}$ is the strain rate; σ_0 is the initial yield stress; C and p is strain rate constant; ε_p^{eff} is effective plastic strain; E_p is the plastic hardening modulus; β is hardening coefficient. For $\beta = 0$ and $\beta = 1$, kinematic and isotropic hardening is obtained, respectively. It is noted that the failure criterion is defined by ε_p^{eff}, and the damaged element is deleted from the model when it reaches the predetermined value.

2.3.3. Validation of Material Models

According to NEI07-13 [2], the accuracy of the constitutive models can be judged on a review of the sample validation cases (against test results). Based on our previous work, simulation analysis of 1/7.5 scale aircraft impact test against SC and RC panels with different thickness was carried out [18]. Details of the experimental study of 1/7.5 scale model of aircraft and RC and SC panels with different thickness were provided in the previous literatures [19,20]. The simulation results in terms of damage modes of panels, velocity time-history curves of engine, and damage to aircraft correlated well with the experimental results, especially for constitutive concrete model of Winfrith [18]. Therefore, the level of accuracy of the constitutive models of the above concrete and steel had been effectively validated. In this study, we continue to use the same constitutive models of

concrete and steel to conduct simulation for the response of SC containment subjected to impact of a large commercial aircraft.

2.3.4. Material Properties of SC Containment

Due to sensitivity analysis of material parameters of SC containment, the strength grades of concrete are selected to be C45, C50, C55, and C60, the strength grades of steel plate are set to be Q235 and Q335, and the rebar is HRB400. For dynamic analysis of impact effects on structure, an increase of strength due to the high strain rate involved in the deformation process is appropriate. In general, the static design strength values should be increased by using dynamic increase factors (DIFs) according to NEI 07-13 [2]. The material properties of concrete, steel plate, and rebar defined in SC containment for the FE analysis are listed in Tables 2 and 3, respectively.

Table 2. Material properties of concrete.

Strength Grade	Density (kg/m^3)	Young's Modulus (GPa)	Poisson's Ratio	Compressive Strength (MPa)	Tensile Strength (MPa)	Aggregate Radius (mm)
C45	2400	34	0.2	42.6	3.6	15
C50	2400	35	0.2	46.7	3.8	15
C55	2400	36	0.2	51.0	4.0	15
C60	2400	36.5	0.2	55.0	4.1	15

Table 3. Material properties of steel plate and rebar.

Strength Grade	Density (kg/m^3)	Young's Modulus (GPa)	Poisson's Ratio	Yield Strength (MPa)
HRB400	7800	206	0.3	440
Q235	7800	206	0.3	300
Q335	7800	206	0.3	430

3. Results and Discussion

Firstly, numerical analysis of evaluating the impact resistant performance of full SC and half SC containment is performed. Subsequently, sensitivity analysis is conducted to evaluate the effect of related parameters on the behavior of full SC containment. These parameters include strength grades of concrete and steel plate, thickness of concrete wall, and steel plate. The impact response is obtained under the impact pressure applied on the middle of the cylinder, as illustrated in Figure 3a.

3.1. Comparison Analysis of Different Types of SC Containment

In this section, the impact resistant behavior of SC containment with different types is investigated. Three models as mentioned in Section 2.2 are considered, which the thickness of cylinder and dome with concrete strength grade C50 is 1.0 m, and the thickness of Q335 steel plate is 20 mm.

The maximum displacement occurs at the location of the fuselage impacted zone, and the maximum displacement time history of a node located at the center of the impact area is plotted in Figure 6. It is obtained that the displacement amplitude of model I, II, and III is 11.52, 16.56, and 46.86 cm, respectively. Hence, it is found that the displacement amplitude of model I and model II is 75.4% and 64.7% lower than that of model III, respectively. Additionally, the time-history curves of maximum plastic strain of concrete are plotted in Figure 7. The peak plastic strain for model I, II and III is found to be 9.27×10^{-4}, 1.27×10^{-3}, and 2.32×10^{-3}, respectively. Further, Figure 8 shows the contours for the maximum plastic strain, and it is evident that the maximum plastic strain occurs at the location of

fuselage and wing impacted zone. In summary, it is obvious that the displacement and plastic strain response of model III is the largest, while that of model I is significantly reduced, which means that full SC containment can effectively reduce the impact response.

As for the local concrete damage caused by aircraft impact, as shown in Figure 8, the concrete around impact zone of model III changed to be plastic state, and there is a large area of concrete debris falling off on the rear face of cylinder. However, the concrete near the impact zone of model I and II only enters to be plastic state without any spalling and scabbing. In addition, local damage to the above three models can be quantitatively analyzed from a perspective of energy transition during the impact process. The time histories of internal energy of concrete and total energy of containment are plotted in Figure 9. It is observed that the above energy of model I is the smallest, the model II is secondly, and the model III is the largest. These results indicate that model III has caused the most serious damage, and the degree of damage for model I is the most slight. From the above comparison, it can be concluded that the impact resistant performance of full SC containment is better than that of half SC containment, and the steel plate located at outer face of containment is better than that at inner face for half SC containment. Accordingly, it should be noted that full SC containment (model I) is selected as the subject in the following sensitivity analysis of material and geometric parameters, due to the best performance of impact resistance.

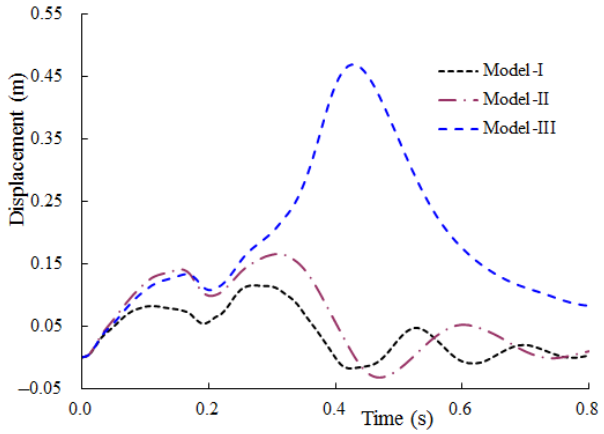

Figure 6. Max displacement time-history of containment.

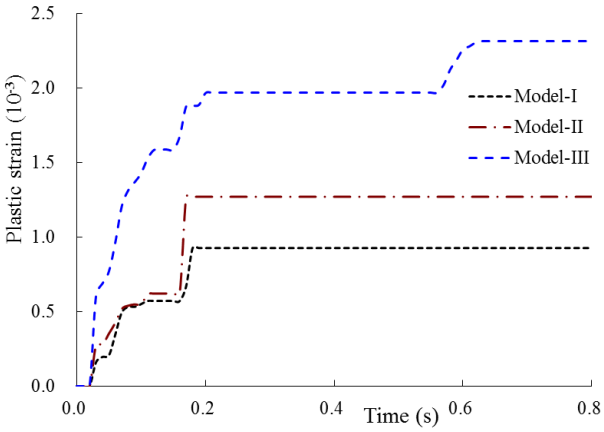

Figure 7. Max plastic strain time-history of concrete.

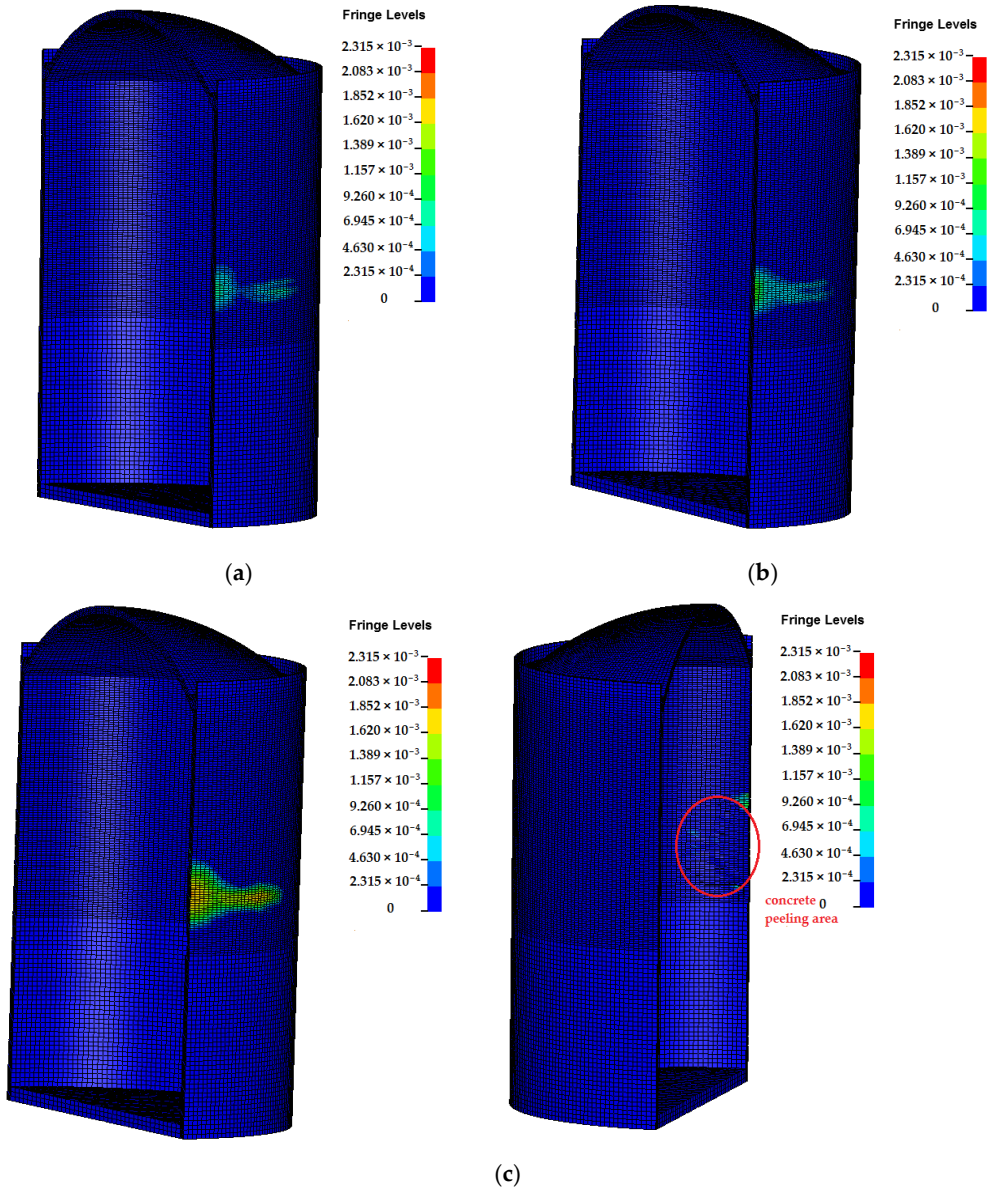

Figure 8. Max plastic strain of concrete for different models. (**a**) Model I; (**b**) Model II; (**c**) Model III.

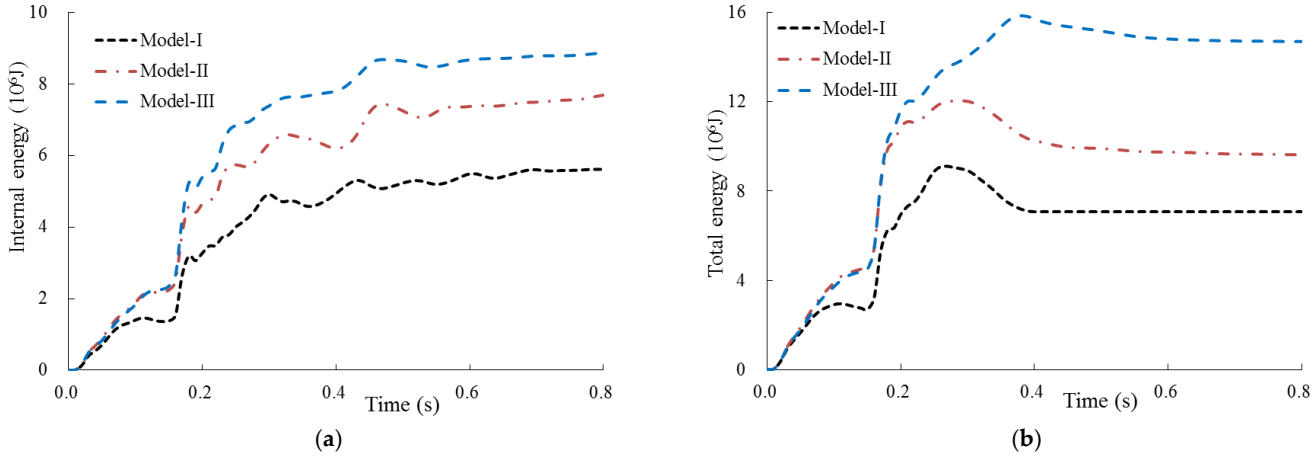

Figure 9. The internal energy of concrete and total energy of containment for different models. (**a**) Internal energy; (**b**) Total energy.

3.2. Sensitivity Analysis of Different Concrete Strength Grades

In this section, the influence of different concrete strength grades on the ability of full SC containment to withstand impact was analyzed. For full SC containment with Q335 steel plate whose thickness is 20 mm, we investigated two cases with respect to the variety of concrete thickness.

3.2.1. Full SC Containment with Thickness of 0.9 m

For relatively thin full SC containment, which the thickness of cylinder and dome is 0.9 m, three concrete strength grades of C50, C55, and C60 are considered herein. Figure 10 shows contours of the maximum impact displacement and concrete peeling area. It can be seen that C50 concrete at the front and rear face of the fuselage impacted area falls off, local penetration occurs, and the steel plates at the inner and outer sides turn to be plastic state without tearing. However, for the impact area of C55 and C60 concrete, only one layer of concrete element (Note: divided into four layers along the thickness direction) at the rear face falls off. Additionally, the influence of concrete strength grade on the impact displacement and plastic strain of concrete is shown in Figures 11 and 12, respectively. It is observed that the displacement and plastic strain response of C50 concrete are apparently enlarged, and both decrease sharply with the enhancing of concrete strength grade. The peak displacement of containment corresponding to concrete strength grade of C50, C55, and C60 is 41.03, 18.49, and 16.70 cm, respectively. Similarly, the peak plastic strain of C50, C55, and C60 concrete is 4.71 $\times$ 10^{-3}, 1.16 $\times$ 10^{-3}, and 1.00 $\times$ 10^{-3}, respectively. Therefore, compared with full SC containment of concrete strength grade C50, the peak displacement and plastic strain of C55, C60 are effectively reduced by 55.0%, 59.3%, and 75.3%, 78.8%, respectively. The above comparison results indicate that the enhancing of concrete strength grade can effectively control the impact response and local concrete damage of full SC containment with thickness of 0.9 m.

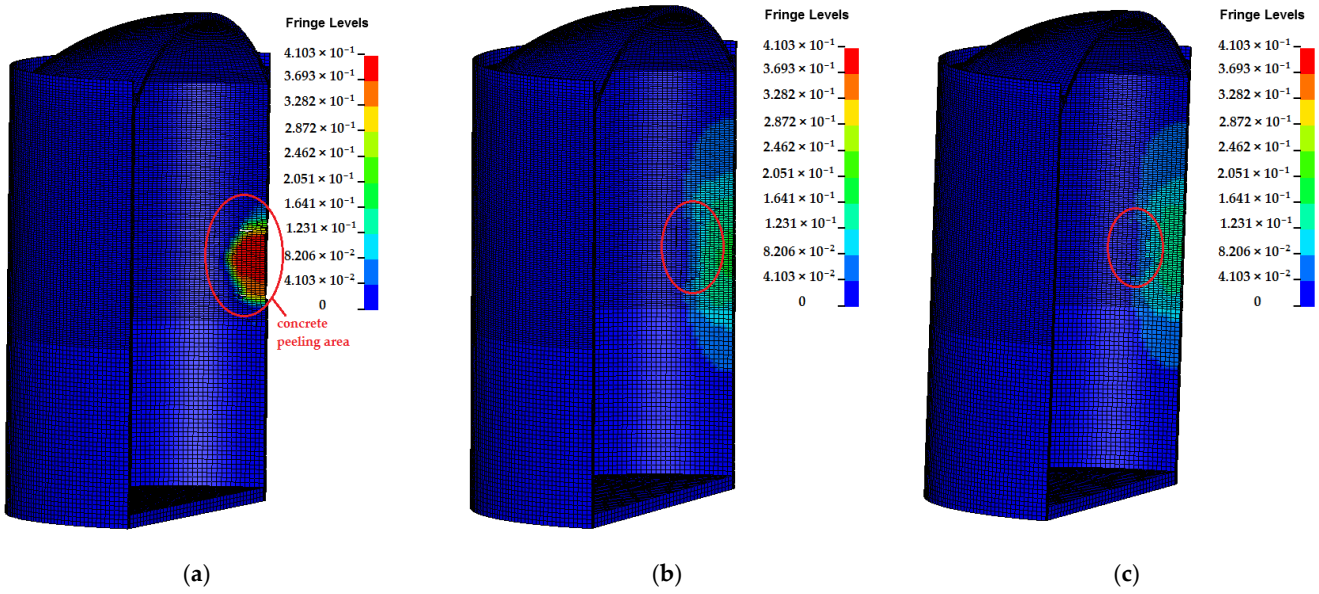

Figure 10. Contours of the maximum impact displacement and concrete peeling off area of full SC containment. (**a**) C50; (**b**) C55; (**c**) C60.

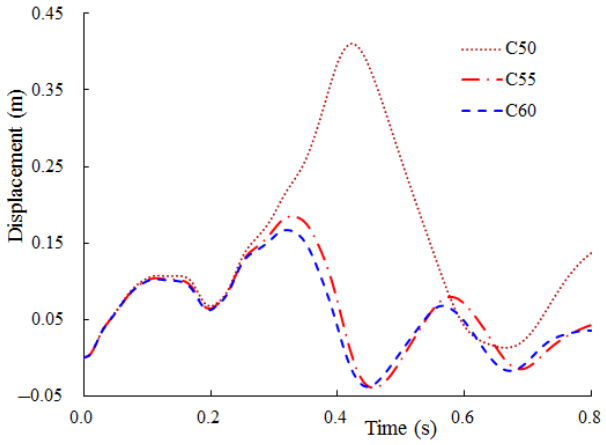

Figure 11. Max displacement time-history of containment.

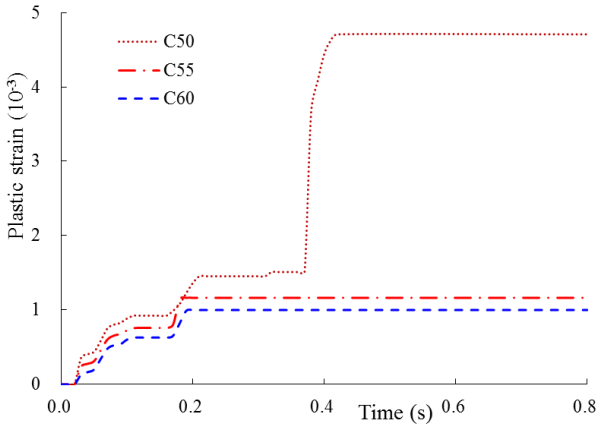

Figure 12. Max plastic strain time-history of concrete.

3.2.2. Full SC Containment with Thickness of 1.0 m

For full SC containment with thickness of 1.0 m, four concrete strength grades of C45, C50, C55, and C60 are considered herein. The time history curves of maximum displacement and plastic strain of impact area are shown in Figures 13 and 14, respectively. As shown in Figure 13, the displacement time history curves have the same trend, and peak displacement decreases slightly with the enhancing of concrete strength grade, which the peak displacement for full SC containment of C45, C50, C55, and C60 is 11.90, 11.52, 11.28, and 11.12 cm, respectively. These results show that concrete strength grade has only a slight influence on the impact displacement of this containment, which means that there is not much advantage to enhance the concrete strength grade for decreasing the impact displacement response. As shown in Figure 14, it is found that along with the enhancing of concrete strength grade, the maximum plastic strain of concrete is descending, among which the plastic strain of C60 concrete decreases significantly compared to that of C45. Specifically, the peak plastic strain of C50, C45, C55, and C60 concrete is 1.14×10^{-3}, 0.93×10^{-3}, 0.90×10^{-3}, and 5.48×10^{-3}, respectively.

Moreover, the time histories of internal energy of concrete and total energy of containment with different strength grades are plotted in Figure 15. It is observed that the internal energy and total energy decreases with the enhancing of concrete strength grade, which is consistent with the decrease of the above impact response.

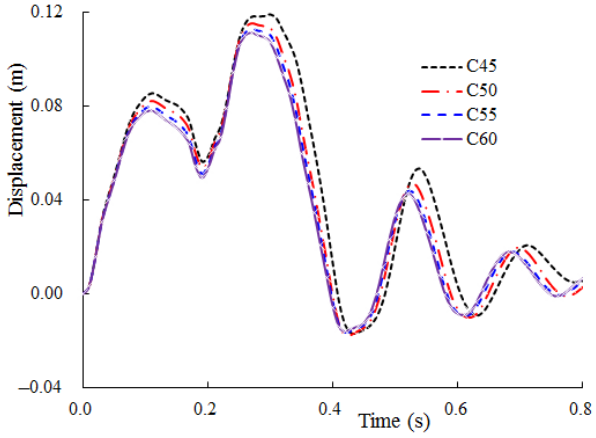

Figure 13. Max displacement time-history of containment.

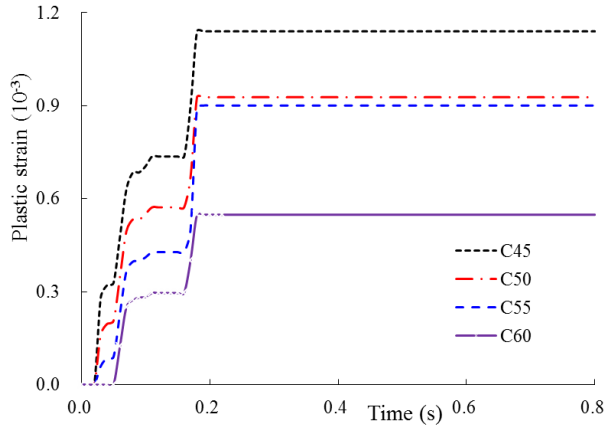

Figure 14. Max plastic strain time-history of concrete.

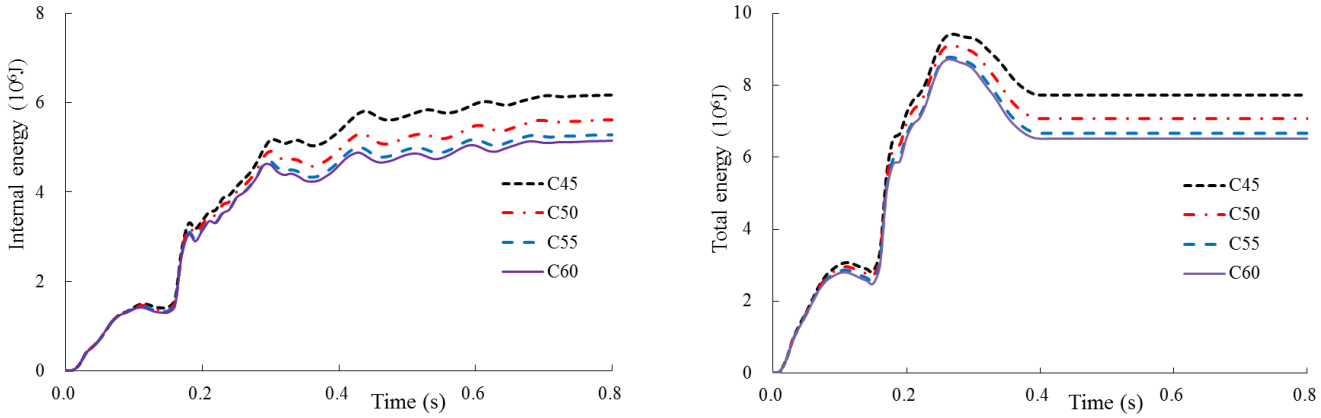

Figure 15. The internal energy of concrete and total energy of containment for different concrete strength grades. (**a**) Internal energy; (**b**) Total energy.

3.3. Sensitivity Analysis of Different Thickness of Steel Plate

In this section, to study the steel plate thickness effect in resisting the impact load, impact analysis of full SC containment with concrete strength grade of C50 for two cases with respect to the variety of concrete thickness was conducted independently.

3.3.1. Full SC Containment with Thickness of 0.9 m

For relatively thin full SC containment, three thicknesses of Q335 steel plates are considered herein, i.e., 18, 20, and 22 mm. As for the local damage zone, it can be seen from Figure 16 that a large area of concrete on the front and rear face of the impact zone falls off and expresses penetration for full SC containment with steel plate whose thickness is 18 mm. However, only local penetration occurs for full SC containment with steel plate whose thickness is 20 mm. For full SC containment with steel plate whose thickness is 22 mm, only one layer of concrete element on the rear face of impact zone falls off. Additionally, it can be seen from Figures 17 and 18 that the maximum displacement, residual displacement and the maximum plastic strain of steel plate at the impact zone decrease greatly with the increasing of steel plate thickness. Further, it is obtained that the peak displacement and plastic strain of steel plate with thickness of 18, 20, 22 mm are 94.19, 41.03, 18.02 cm and 16.04 $\times$ 10^{-3}, 9.87 $\times$ 10^{-3}, 2.51 $\times$ 10^{-3}, respectively. Furthermore, the integrity of the above steel plates with different thickness is not damaged.

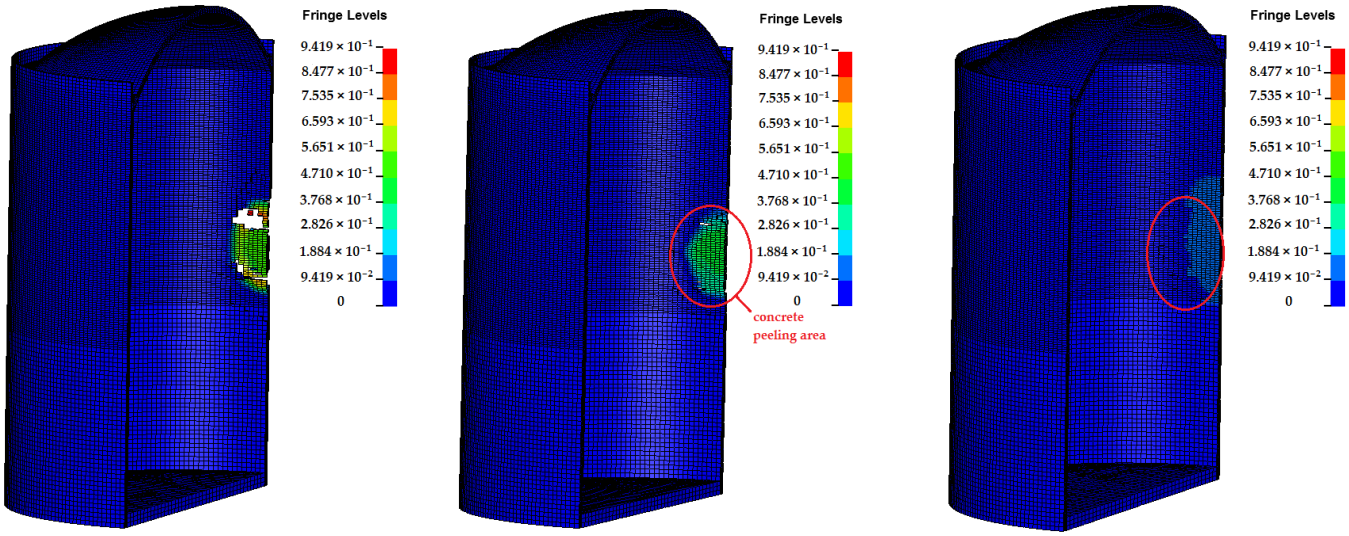

Figure 16. Contours of the maximum impact displacement and concrete peeling off area of full SC containment. (**a**) t = 18 mm; (**b**) t = 20 mm; (**c**) t = 22 mm.

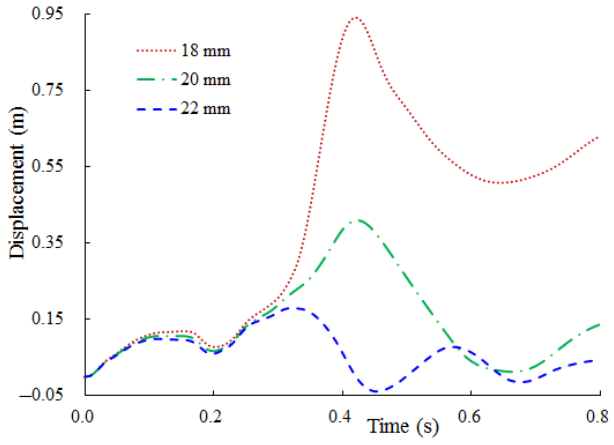

Figure 17. Max displacement time-history of containment.

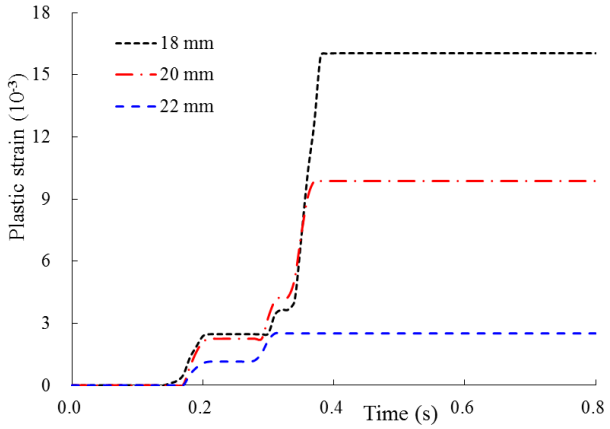

Figure 18. Max plastic strain time-history of steel plate.

The above results illustrate that the thickness of steel plate plays an important role in the ability of this containment to withstand impact. Comparison of internal energy for steel plate corresponding to different thickness is plotted in Figure 19. It shows that the thicker the steel plate becomes, the less internal energy is absorbed. Quite specially, the internal energy absorbed by 18 mm thickness steel plate is the extremely largest, which is consistent with the largest impact response of displacement and plastic strain. In other words, its internal energy decreases significantly with the increasing of thickness, corresponding to the decrease of structural impact response.

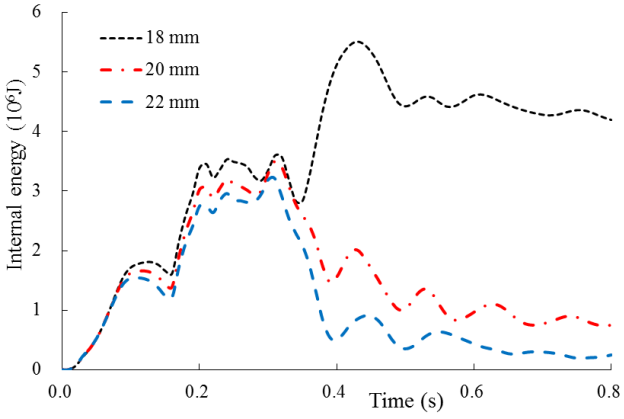

Figure 19. The internal energy time-history of steel plates with different thickness.

In conclusion, the increasing of steel plate thickness can effectively mitigate the structural impact response and local concrete damage for full SC containment with thickness of 0.9 m, which plays a good role in protecting full SC containment from aircraft crash.

3.3.2. Full SC Containment with Thickness of 1.0 m

For relatively thick full SC containment with Q335 steel plate whose thickness is 16, 18, 20, and 22 mm, sensitivity analysis of the above full SC containments is carried out herein. The variation of maximum displacement of containment with respect to time is plotted in Figure 20. It is observed that the four impact displacement time-history curves have the same trend, and the peak displacement corresponding to steel plate whose thicknesses is 16, 18, 20, and 22 mm is 13.38, 12.26, 11.52, and 10.93 cm, respectively. It means that the reduction ratio of peak displacement is only 18.3%, when the thickness of steel plate is increased from 16 to 22 mm. From this result, it is clear that the increasing of steel plate thickness has no significant effect on mitigating the impact displacement response. In addition, Figure 21 shows the influence of steel plate thickness on its plastic strain. A large plastic strain reduction with the increasing of steel plate thickness is observed. Further, it is

obtained that the peak plastic strain of steel plate with thickness of 16, 18, 20, and 22 mm is 1.75×10^{-3}, 5.59×10^{-4}, 2.47×10^{-3}, and 0, respectively. Besides, for full SC containment with the steel plate thickness of 20 mm, the strength grade of steel plate is reduced from Q335 to Q235. Through the comparison as shown in Figures 20 and 21, it can be confirmed that the decreasing of strength grade of steel plate has a minimal effect on the displacement response, but the plastic strain of steel plate increases significantly.

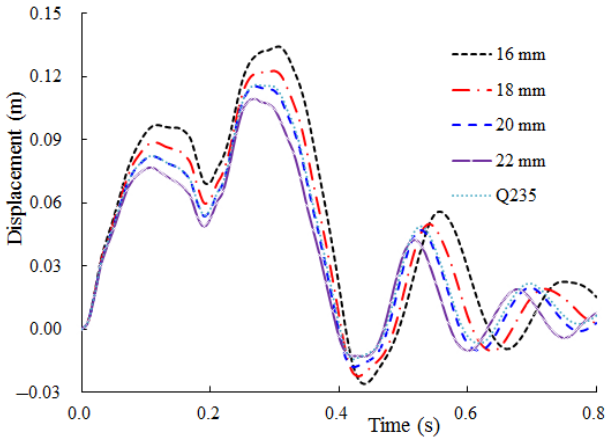

Figure 20. Max displacement time-history of containment.

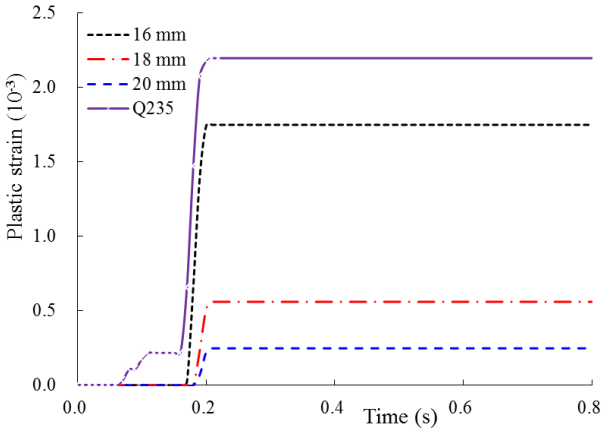

Figure 21. Max plastic strain time-history of steel plates.

In summary, for relatively thick full SC containment, although the increasing of steel plate thickness has not much advantage for decreasing the displacement response, it can effectively reduce its plastic strain. In addition, the decreasing of strength grade of steel plate may obviously increase its plastic strain.

3.4. Sensitivity Analysis of Different Thickness of Concrete

In this section, in order to investigate the influence of concrete thickness on the capacity of full SC containment, numerical analysis includes several cases of full SC containment with respect to the variety of concrete thickness and concrete strength grade.

3.4.1. Full SC Containment with Thickness of 0.8 m

For full SC containment whose thickness of Q335 steel plate is 20 mm, the concrete strength grade is C50 and the thickness of cylinder and dome is 0.8 m, impact analysis is performed herein. Contours of the maximum impact displacement and failure modes of concrete and steel plate are plotted in Figure 22. It is observed that concrete in the fuselage impacted zone is completely crushed and peeled off, and the inner steel plate is torn. The maximum displacement time histories of inner and outer steel plate at the impact zone

is plotted in Figure 23. It is seen that the displacement of the inner and outer plate is the same at the initial moment till 0.35 s, and then the displacement of inner plate is much larger than that of outer plate. The peak displacement of inner steel plate is 3.17 m in the impact direction. Moreover, the outer steel plate at the region of the impact is intact, but has yielded, which the peak and residual displacement is 1.67 and 1.41 m, respectively. In a word, the above results indicate that this full SC containment cannot resist the impact load. So, the concrete thickness is increased for the subsequent analysis.

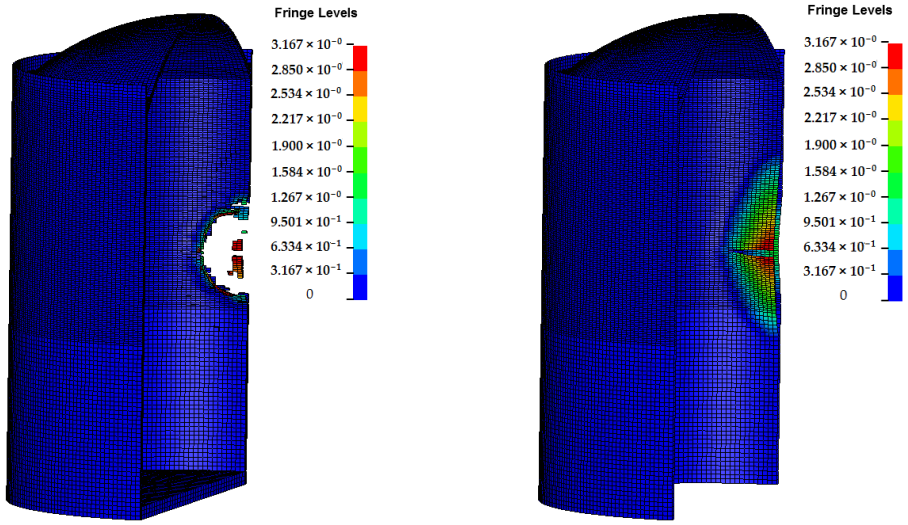

(**a**) (**b**)

Figure 22. Contours of the maximum impact displacement and failure modes. (**a**) Concrete; (**b**) Steel plate.

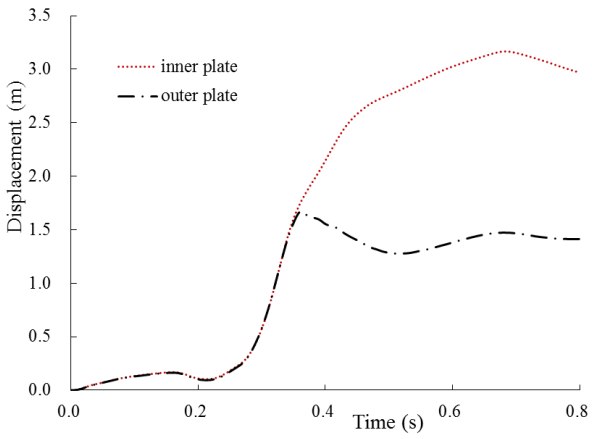

Figure 23. Max displacement time-history of steel plate.

3.4.2. Full SC Containment with Thickness of 0.9–1.1 m

For full SC containment which the thickness of steel plate is 20 mm, and the concrete strength grade is C50, sensitivity analysis for the thickness of concrete 0.9, 1.0, and 1.1 m is conducted herein. The comparison of maximum displacement and maximum plastic strain of concrete in cases of different thickness is plotted in Figures 24 and 25, respectively. The peak displacement of containment and the peak plastic strain of concrete are summarized in Table 4. It is found that the peak displacement and plastic strain corresponding to the concrete thickness of 1.0 m, 1.1 m is reduced by 71.9%, 74.9%, and 86.7%, 80.3%, compared with that of full SC containment with thickness of 0.9 m. Moreover, for full SC containments with thickness of 1.0 m and 1.1 m subjected to impact load, no scattered debris

is observed, while the containment with thickness of 0.9 m shows some scattered debris of concrete around the impact region and local penetration occurs, as plotted in Figure 10a. It is worth noting that all the steel plates of the above full SC containments are intact. Based on these comparison results, it is confirmed that the structural impact response (i.e., displacement, plastic strain, and local concrete damage) of full SC containment can be reduced significantly by the increasing of concrete thickness, which means that concrete thickness affects the impact response of full SC containment prominently.

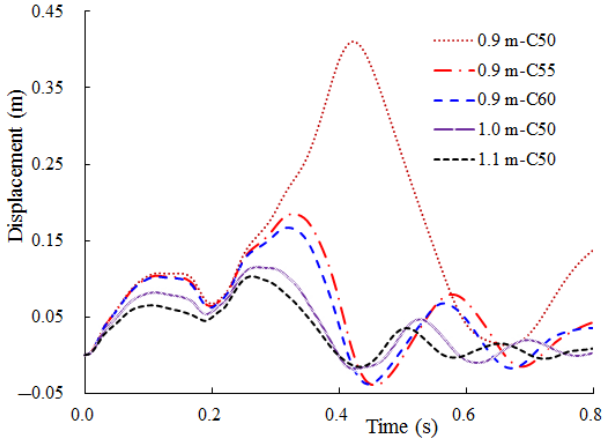

Figure 24. Max displacement time-history of containment.

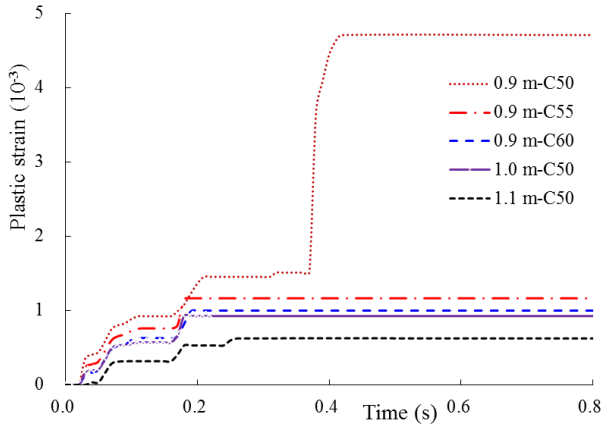

Figure 25. Max plastic strain time-history of concrete.

Table 4. The peak displacement, plastic strain, internal energy, and total energy.

Type	Displacement (cm)	Plastic Strain	Internal Energy (J)	Total Energy (J)
0.9 m-C50	41.03	4.71×10^{-3}	8.40×10^{6}	15.80×10^{6}
1.0 m-C50	11.52	9.27×10^{-4}	5.62×10^{6}	9.11×10^{6}
1.1 m-C50	10.31	6.25×10^{-4}	4.40×10^{6}	7.72×10^{6}
0.9 m-C55	18.49	1.16×10^{-3}	8.02×10^{6}	12.39×10^{6}
0.9 m-C60	16.70	1.00×10^{-3}	7.61×10^{6}	11.77×10^{6}

Additionally, in order to comprehensively evaluate the effect of concrete strength grade and concrete thickness on the impact resistant behavior of full SC containment, the simulation results calculated by full SC containment with the thickness of 0.9 m and the concrete strength grade of C55 and C60 are also supplied in Figures 24–26 and Table 4.

As summarized in Table 4, the comparison results indicate that the peak displacement, plastic strain, internal energy of concrete, and total energy of containment decrease with the increasing of concrete thickness and the enhancing of concrete strength grade, but the increasing of concrete thickness can reduce the above results more considerably than the enhancing of concrete strength grade. For instance, the peak displacement corresponding to concrete thickness of 1.0 and 1.1 m is reduced by 71.9% and 74.9%, and the peak displacement corresponding to concrete strength grade of C55 and C60 is reduced by 55.0% and 59.3%, compared with that of full SC containment whose concrete thickness is 0.9 m and concrete strength grade is C50. Therefore, it can be concluded that the increasing of concrete thickness is more effective in reducing the impact displacement response and plastic damage of concrete than the enhancing of concrete strength grade.

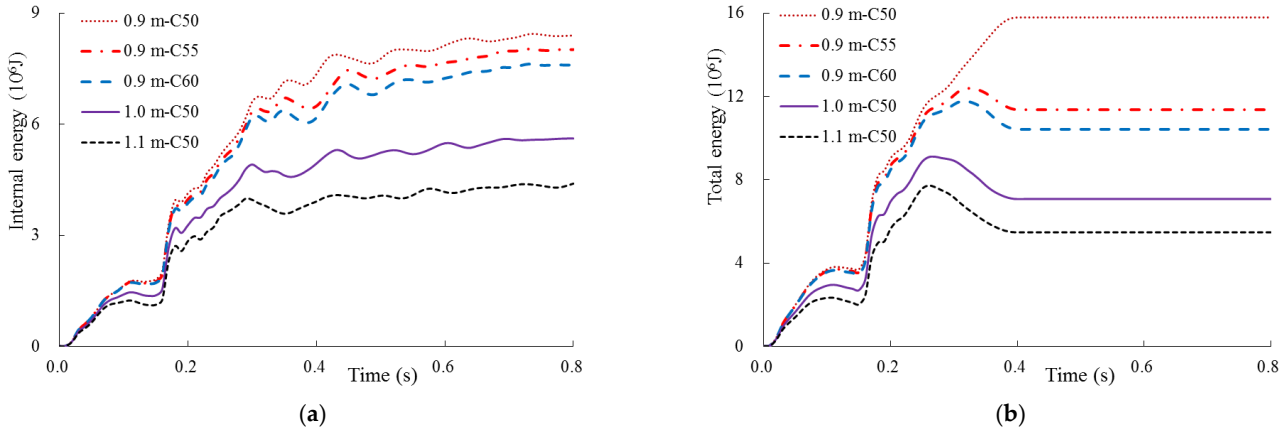

(**a**) (**b**)

Figure 26. The internal energy of concrete and total energy of containment with different thickness and concrete strength grade. (**a**) Internal energy; (**b**) Total energy.

4. Conclusions

The FE models of full SC and half SC containment were created, and then sensitivity analysis of full SC containment against a large commercial aircraft crash had been performed to investigate the influence of the related parameters on the impact response of containment, based on the force time-history analysis method. Some conclusions are derived as follow.

(1) The impact resistant performance of full SC containment is better than that of half SC containment. For half SC containment, the steel plate located at outer face of containment is better than that at inner face.

(2) For relatively thin full SC containment, it is more effective in reducing the impact response and concrete damage by the enhancing of concrete strength grade or the increasing of steel plate thickness comparing to thicker full SC containment. The impact response of displacement and plastic strain both decrease sharply with the enhancing of concrete strength grade. The steel plate thickness plays an important role in the capacity of this containment to withstand impact load, the peak displacement is approximately reduced by 55% and 80%, when the steel plate thickness is increased from 18 to 20 and 22 mm, respectively.

(3) For the thicker full SC containment, it is clear that there is not much advantage to enhance the concrete strength grade and increase the steel plate thickness for decreasing the impact displacement response. For example, the reduction ratio of peak displacement is only 6.6%, when the concrete strength grade is improved from C45 to C60, and the reduction ratio corresponding to the steel plate thickness increased from 16 to 22 mm is only 18.3%. Of course, the increasing of steel plate thickness can effectively reduce its plastic strain, and the decreasing of strength grade of steel plate may obviously increase its plastic strain.

(4) The structural impact response (i.e., displacement, plastic strain and local concrete damage) of full SC containment can be reduced significantly by the increasing of concrete thickness. Concrete thickness plays a decisive role on the improvement of impact resistance and is more effective than the enhancing of concrete strength grade. Specially, full SC containment with thickness of 0.8 m cannot resist the impact load, and the reduction ratio of peak displacement reaches 71.9%, when concrete thickness is increased from 0.9 to 1.0 m.

Author Contributions: Conceptualization, X.Z. and G.L.; methodology, X.Z. and J.L.; software, X.Z.; validation, X.Z.; writing—original draft preparation, X.Z. and J.L.; writing—review and editing, G.L. and R.P.; data curation, L.L. All authors have read and agreed to the published version of the manuscript.

Funding: This research was funded by National Science and Technology Major Project of advanced technology research on structural health inspection and evaluation of nuclear power plants (Grant Number: 2018ZX06002008).

Institutional Review Board Statement: Not applicable.

Informed Consent Statement: Not applicable.

Data Availability Statement: Not applicable.

Conflicts of Interest: The authors declare no conflict of interest.

References

1. 10CFR50.150. *Aircraft Impact Assessment*; Nuclear Regulatory Commission: Washington, DC, USA, 2009.
2. NEI07-13. *Methodology for Performing Aircraft Impact Assessments for New Plant Designs*; Rev 8P; Prepared by ERIN Engineering & Research; Nuclear Energy Institute: Walnut Creek, CA, USA, 2011.
3. HAF102. *Design Safety Regulations for Nuclear Power Plants*; National Nuclear Safety Administration: Beijing, China, 2016.
4. Riera, J.D. On the stress analysis of structures subjected to aircraft impact forces. *Nucl. Eng. Des.* **1968**, *8*, 415–426. [CrossRef]
5. Abbas, H.; Paul, D.K.; Godbole, P.N.; Nayak, G.C. Reaction-time response of aircraft crash. *Comput. Struct.* **1995**, *55*, 809–817. [CrossRef]
6. Arros, J.; Doumbalski, N. Analysis of aircraft impact to concrete structures. *Nucl. Eng. Des.* **2007**, *237*, 1241–1249. [CrossRef]
7. Sugano, T.; Tsubota, H.; Kasai, Y.; Koshika, N.; Orui, S.; von Riesemann, W.A.; Bickel, D.; Parks, M. Full-scale aircraft impact test for evaluation of impact force. *Nucl. Eng. Des.* **1993**, *140*, 373–385. [CrossRef]
8. Tennant, D.; Mould, J.; Vaughan, D.; Levine, H. Rapid evaluation of buildings and infrastructure to accidental and deliberate aircraft impact. *Nucl. Eng. Des.* **2014**, *269*, 142–148. [CrossRef]
9. Zhang, T.; Wu, H.; Fang, Q.; Gong, Z.M. Influences of nuclear containment radius on the aircraft impact force based on the Riera function. *Nucl. Eng. Des.* **2015**, *293*, 196–204. [CrossRef]
10. Jiang, H.; Chorzepa, M.G. Aircraft impact analysis of nuclear safety-related concrete structures: A review. *Eng. Fail. Anal.* **2014**, *46*, 118–133. [CrossRef]
11. Lee, K.; Han, S.E.; Hong, J.-W. Analysis of impact of large commercial aircraft on a prestressed containment building. *Nucl. Eng. Des.* **2013**, *265*, 431–449. [CrossRef]
12. Frano, R.L.; Forasassi, G. Preliminary evaluation of aircraft impact on a near term nuclear power plant. *Nucl. Eng. Des.* **2011**, *241*, 5245–5250. [CrossRef]
13. Thai, D.K.; Kim, S.E. Safety assessment of a nuclear power plant building subjected to an aircraft crash. *Nucl. Eng. Des.* **2015**, *293*, 38–52. [CrossRef]
14. Shin, S.S.; Hahm, D.; Park, T. Shock vibration and damage responses of primary auxiliary buildings from aircraft impact. *Nucl. Eng. Des.* **2016**, *310*, 57–68. [CrossRef]
15. Mullapudi, T.; Summers, P.; Moon, I.-H. Impact Analysis of Steel Plated Concrete Wall. *Struct. Congr.* **2012**, *2012*, 1881–1893. [CrossRef]
16. Liu, J.; Han, P. Numerical analysis of a shield building subjected to a large commercial aircraft impact. *Shock Vib.* **2018**, *2018*, 7854969.
17. Sadiq, M.; Khaliq, W.; Ilyas, M.; Khushnood, R.A.; Khan, S.A.; Rong, P. Analysis of full-scale aircraft impact to reinforced concrete and steel plate reinforced concrete multiple barriers protecting nuclear power plants. *Structures* **2020**, *27*, 732–746. [CrossRef]
18. Sadiq, M.; Yun, Z.X.; Rong, P. Simulation analysis of impact tests of steel plate reinforced concrete and reinforced concrete slabs against aircraft impact and its validation with experimental results. *Nucl. Eng. Des.* **2014**, *273*, 653–667. [CrossRef]

19. Tsubota, H.; Koshika, N.; Mizuno, J.; Sanai, M.; Peterson, B.; Saito, H.; Imamura, A. Scale model tests of multiple barriers against aircraft impact: Part 1. Experimental program and test results. In Proceedings of the Transactions of the 15th International Conference on Structural Mechanics in Reactor Technology (SMiRT-15), Seoul, Korea, 15–20 August 1999.
20. Mizuno, J.; Koshika, N.; Morikawa, H.; Fukuda, R.; Wakimoto, K. Investigations on impact resistance of steel plate reinforced concrete barriers against aircraft impact Part 1: Test program and results. In Proceedings of the Transactions of the 18th International Conference on Structural Mechanics in Reactor Technology, Beijing, China, 7–12 August 2005; pp. 2566–2579.
21. Westinghouse Electric Corporation. *AP1000 Design Control Document*; Rev.19; Westinghouse Electric Corporation: Cranberry Township, PA, USA, 2011.
22. Huang, T.; Zhang, T.; Dong, Z.; Wu, H.; Fang, H. An analysis of the dynamic response of nuclear containment under the impact of a large commercial aircraft. *J. Vib. Shock* **2018**, *37*, 8–14.
23. Ls-Dyna LSTC. *LS-DYNA Keyword User's Manual*; Livermore Software Technology Corporation (LSTC): Livermore, CA, USA, 2010.
24. Ottosen, N.S. *Failure and Elasticity of Concrete. Danish Atomic Energy Commission*; RISOE: Roskilde, Denmark, 1975; ISBN 8755003540.